
Vibration control and preliminary evaluation of a piezoelectric actuator for use as a force-feedback device

Gaston M'boungui¹, Betty Lemaire-Semail², Frederic Giraud²

1. Department of Electrical Engineering

Tshwane University of Technology

Private bag 7680, Pretoria 0001, Republic of South Africa

2. Laboratoire d'Électrotechnique et d'Électronique de Puissance de Lille

Université Lille 1

IRCICA, 50 av. Halley, 59650 Villeneuve d'Ascq, France

ABSTRACT. As a solution to cope with the lack of compactness and simplicity often encountered in haptic interfaces, we propose a device based on friction coefficient control principle. This device includes polarised piezoceramics well adjusted and glued to a 64x38x3 mm copper-beryllium plate supported by four legs. Then, properly energised around a resonant frequency, with legs at antinodes, a stationary wave is created in the plate. Variable friction forces between the legs and the plane substrate are created by the control of the wave amplitude, according to electro-active lubrication. So the user obtains force feedback by holding the plate, and moving it on a plane substrate, as he could do with a mouse interface. Preliminary psychophysical evaluation trends to assess the validity of the device as a force feedback interface.

RÉSUMÉ. Comme solution au manque de compacité et de simplicité observé au niveau de nombreuses interfaces haptiques, nous proposons un dispositif de conception simple fonctionnant sur le principe de régulation du coefficient de frottement. Cette structure est constituée d'une plaque en cuivre-béryllium de dimension 64x38x3 mm sur laquelle sont collées à l'époxy des céramiques piézoélectriques PZT convenablement agencées. Cette plaque tient sur quatre pieds chacun à l'extrémité plane. Ainsi, une alimentation électrique adéquate du dispositif autour de sa fréquence de résonance crée une onde stationnaire dont on a choisi deux ventres pour positionner les pieds. Dès lors une force de frottement variable entre les pieds et un substrat en acier par exemple est obtenue par le contrôle de l'amplitude vibratoire en harmonie avec le principe de la lubrification électro active. Comme résultat, un usager perçoit un effort en tenant la plaque avec les doigts de la main et en déplaçant cette plaque sur le substrat plan comme il le ferait avec une souris d'ordinateur. Une première évaluation psychophysique tend à valider le dispositif comme une interface à retour d'effort.

KEYWORDS: piezoelectric actuator, haptic, electro-active lubrication.

MOTS-CLÉS: actionneur piezoelectrique, haptique, lubrification electro-active.

DOI:10.3166/EJEE.17.9-26 © 2014 Lavoisier

1. Introduction

Many of the tasks in our daily life may be performed with greater efficiency and speed using haptic (tactile and force feedback rendering) assistance (Casiez *et al.*, 2003). Consequently, the use of force feedback to enhance interactive graphics has often been discussed since it's an area of growing interest from the research community and various devices of this field have been developed over many years. On the other hand, available force feedback interfaces are generally complex using a broad range of technologies, even if DC motors are usually used as force rendering actuators. So, as a motivation, in our research, we aimed at designing a compact and simple force feedback device.

This work presents the design and implementation of our proposal which is a passive 2 DoF (two Degree of Freedom) device able to provide different resistant feelings when a user moves it. To realise such a system, we chose to use active lubrication effect (Garbuio and Rouchon, 2006) induced by piezoelectric actuator.

The actuator will first be described: it is based on a vibrating plate fitted with four legs. Then, the principle of active lubrication is reminded in that specific case which leads to a global control of adjustable friction coefficient between the plate and its plan support. This effect is underlined through simulation and experimental results about reactive force obtained with the device. At last, we also introduce preliminary evaluation of the system in use towards its qualification for force feedback rendering. A psychophysical test is described and its results presented.

2. Device

Figure 1 schematically shows the proposed structure. A set of PZT polarised piezo-ceramics of 12x12x1mm are glued on the upside of a copper-beryllium substrate whose size is 64x38x3 mm. On the opposite side (Figure 1), four built in feet support the plate despite of hyperstaticity it implies.

Considering this polarisation, piezo-ceramic electrodes are conveniently supplied by a sinusoidal voltage of some ten Volts to create a standing wave using the piezoelectricity inverse effect with 40.7 kHz driving frequency (resonant frequency). As a result, Figure 2 shows an experimental mapping of the standing waveform obtained in accordance with a Finite Element (FE) analysis that showed a corresponding resonant wave shape and frequency equal to 42.7 kHz. The beryllium and lead Zirconate Titanium (PZT) properties were taken into account in the FE model as well as the ceramics polarisation. The material properties of each material are shown in Table 1.

Table 1. Material properties

	Beryllium	PZT
Young's modulus [GPa]	123	72.6
Poisson ratio	0.3	0.31
Mass density [10^3 kg/m^3]	8.25	7.7
Elements	C3D8	C3D8E
Material Property		Orthotropic

The piezoelectric coupling matrix d [C/N] is also given.

$$d = \begin{bmatrix} 0 & 0 & 0 & 0 & 10.17e-9 & 0 \\ 0 & 0 & 0 & 10.17e-9 & 0 & 0 \\ 13.7e-9 & 13.7e-9 & 13.7e-9 & 0 & 0 & 0 \end{bmatrix}$$

The commercially Abaqus® package was used for the analysis and we believe that including epoxy layer, damping, etc. in the modelling should bring resonant frequencies of 40.7 and 42.7 kHz much closer.

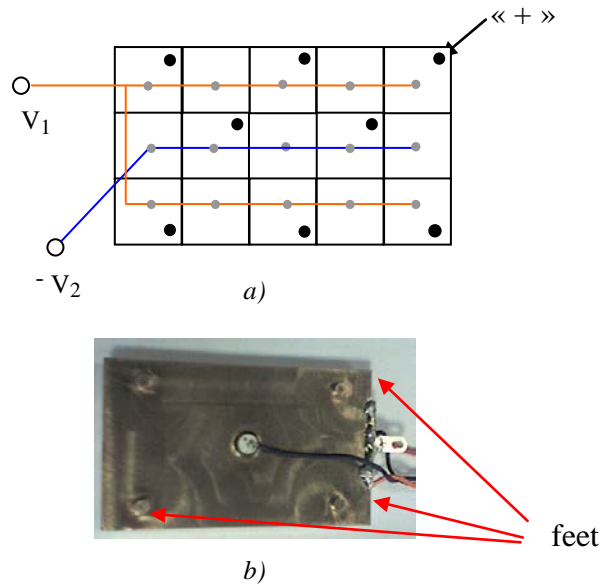
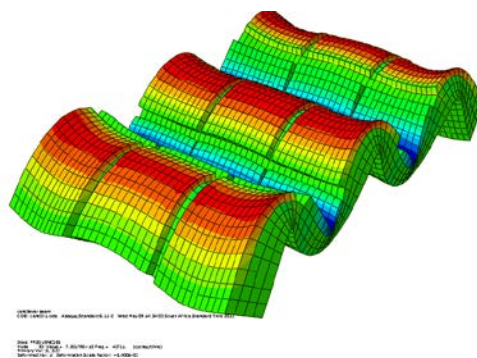


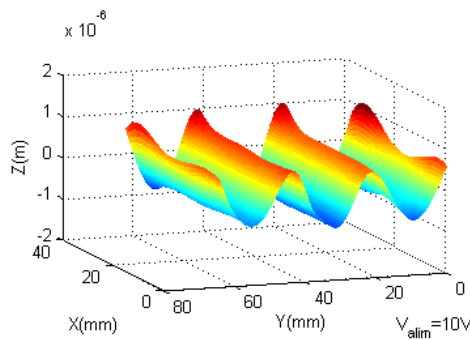
Figure 1. Up and down view of the actuator: a) electrical connection
b) four feet and measurement ceramic location

Earlier some studies have been carried out using a system closed to this structure (Pigache *et al.*, 2006; Le Moal *et al.*, 2000). The main difference is that this plate will only move normally. Indeed, as we will see later, this particular structure is not supposed to move by itself along the tangential direction.

Let's notice that similarity between theoretical and experimental wave shapes in Figure 2 allowed the definition of the feet coordinates, located at the anti-node position in our case. Also, the magnitude in Figure 2a corresponds to an arbitrary value.



a)



b)

Figure 2. Wave shape of the standing wave induced in the plate: a) FEM result
b) experimental result

3. Operating principle

As explained above, the feet are positioned exactly at the antinodes (Figure 3) of the vibrating plate and they are in contact with a plan steel substrate for example.

Therefore, when no voltage is applied to the ceramics, if users move the actuator, they can feel the classical Coulomb friction force acting at the interface feet/substrate.

When voltage is applied to the ceramic electrodes, a standing wave is generated and the friction between feet and substrate is decreased: this happens according to amplitude vibration. As a matter of fact, from a given wave amplitude, an intermittent contact may occur at the interface. Consequently, at the feet base, transitions between stick or slip conditions are created

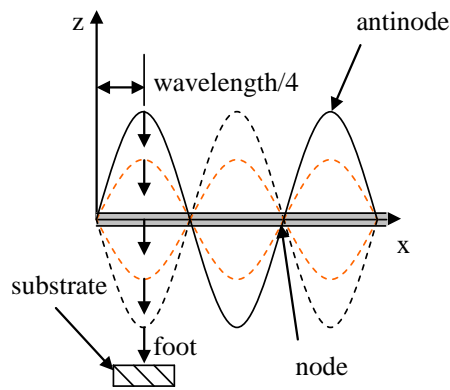


Figure 3. Stationary wave and foot trajectory

4. Stick/slip generation condition

From (Desai *et al.*, 1998) micro-slip is defined as a “Small relative tangential displacement in a contacting area at an interface, when the remainder of the interface in the contacting area is not relatively displaced tangentially”: this means the existence of a region at the feet basis where the surfaces are said to adhere or to slide. In our case, the user’s action leads two surfaces in contact to slide against each other: an elastic (micro-slip) and plastic deformation may occur before macro-slip takes place. Therefore our principle to generate stick-slip conditions will be based on the consideration that for small displacements in z axis, foot/substrate contact presents stick and partial slip zones under a normal load R_n . Furthermore, it is shown on Figure 2 that the plate deformation scale is in micrometer, so we can use an approach based on Coulomb-Orowan model (Figure 4) to interpret friction coefficient (μ) variations.

Figure 4 depicts friction coefficient as a function of δ and the plot is divided approximately in two parts. The first part, relative in tangential stiffness of the contact, is linear and describes the partial slip. Then, from a critical displacement (δ_{crit}) corresponding to total slip, μ is constant.

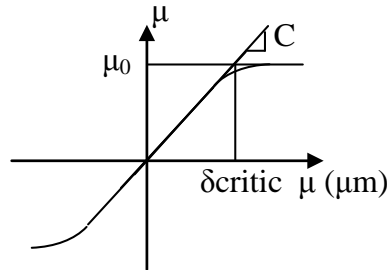


Figure 4. Coulomb-Orowan model

As explained above, the feet are positioned exactly at the antinodes (Figure 3) of the vibrating plate and they are in contact with a plan steel substrate for example. Therefore, when no voltage is applied to the ceramics, if users move the actuator, they can feel the classical Coulomb friction force acting at the interface feet/substrate.

We define δ_{crit} from the following relationship after prior identification of tangential stiffness k_t :

$$\delta_{crit} = \mu_0 \cdot C \cdot R_n = \frac{\mu_0 \cdot R_n}{k_t} \quad (1)$$

Where $C(m/N)$ is the compliance and μ_0 , the maximum friction coefficient at the interface (static friction).

As a consequence, we are able to obtain $\mu(t)$ during the foot/substrate contact time, limited by t_c and t_s which are respectively the contact and separation instants during one period of our vibrating device. We can then write:

$$\text{if } t \in]t_c, t_s[\text{ and } \delta < \delta_c \text{ then } \mu(t) = \frac{\mu_0}{\delta_{crit}} \cdot \delta(t), \quad (2)$$

$$\text{if } t \in]t_c, t_s[\text{ and } \delta > \delta_c \text{ then } \mu = \mu_0 \quad (3)$$

The displacement $\delta(t)$ is computed from the tangential speed integration.

$$\delta(t) = \int_0^t V_t(t) dt \quad (4)$$

where V_t is the relative sliding speed between the two surfaces in contact.

5. Variation of normal and tangential forces

Each foot can be modelled as a mass-spring system and we represented it in Figure 5.

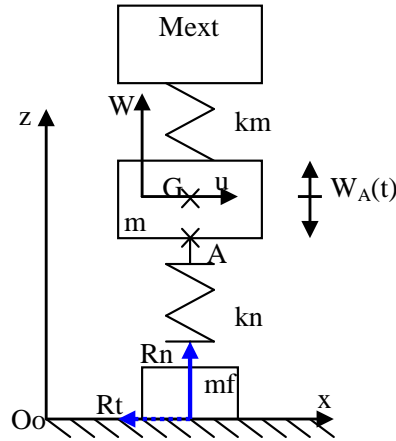


Figure 5. Equivalent mechanical scheme and forces acting on the foot

In Figure 5, M_{ext} represents the load applied on the top of the device to assume pre-stress. This load lies on an elastic element whose stiffness k_m is low enough to consider constant the force F_n due to M_{ext} ($F_n = 9.81M_{ext}$). The mass of the vibrating plate is noted m and the number of feet, n . The foot mass is too low to be considered and its stiffness is k_n . Finally the displacement $w_A(t)$ is imposed by the plate vibrations.

By applying the general dynamic laws to the system and considering that only the foot is storage element of potential energy, we have:

$$\frac{m}{n} \ddot{z}_A = \frac{m}{n} \ddot{w}_A - \frac{F_n}{n} - \frac{m}{n} g + R_n(t) \quad (5)$$

Where, during contact,

$$R_n(t) = k_n (h - z_A(t)) - d_n \dot{z}_G \quad (6)$$

With k_n the elasticity of the foot, h the height of the foot when no pressure is exerted on it and d_n a damping coefficient on the main compression of the foot induced by variation of z_G .

And during separation,

$$R_n(t) = 0 \tag{7}$$

The knowledge of instantaneous reaction $R_n(t)$, which will be a dynamic load, by solving numerically Equation (5) allows us to deduce the tangential force $R_t(t)$. For that aim we use Coulomb's law $R_t = \mu(t)R_n$, with μ the friction coefficient previously defined.

R_t mean value is obtained by integration on a vibrating period.

$$\langle R_t \rangle = \frac{1}{T} \cdot \int_0^T R_t(t) dt \tag{8}$$

From the previous equations, it is possible to compute the behaviour of the actuator for a given wave amplitude, a given tangential speed and a given normal load. The simulation results are given Figure 6.

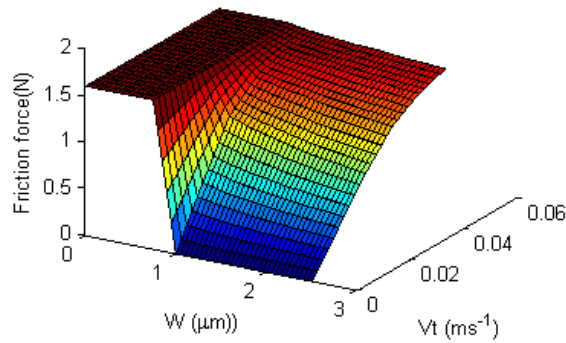


Figure 6. Friction force on the plate for a fixed preload, as a function of wave amplitude and user tangential speed

It is noticeable that from a given amplitude value, friction decreases suddenly. This amplitude value corresponds in fact to the appearance of an intermittent contact between the foot and the substrate. A glass substrate ($\mu_0=.08$) was used for these trials.

Moreover, we can check by the same way the normal pre-load influence thanks to the simulation results given on Figure 7. We can see that the tangential force rises, at exploration speed of 5 cm/s with pre-load addition and decreases when the vibratory amplitude decreases. We can notice that faster the plate is displaced by a user, lower is friction force reduction.

The determination of R_t is a key point for this study and the variations highlighted in Figures 6 and 7 justify the possibility to use this device for force feedback. Indeed, we will have to control the wave amplitude, the two other variables being not suitable for control: the tangential speed will be imposed externally by the user, and the normal pre-load should be imposed once for quite.

6. Control of the vibration amplitude

The control of the vibratory amplitude may be achieved following different approaches. In (Pigache *et al.*, 2005), the wave amplitude control is done thanks to the phase control of the standing wave according to the voltage signal supply. The advantage of this method is its high robustness against resonance frequency variations. One drawback is a lower dynamic behaviour due to the response time imposed by a Phase Locked Loop (PLL).

Another way to control the wave amplitude is to tune the supply frequency around the resonance value. This approach comes from the characteristic frequency – vibratory amplitude which shows that beyond the resonant frequency, the wave amplitude W decreases quasi – linearly, making possible its control (Piecourt and Mazenc, 1995). The method presents the advantage of being easy to implement and the loop dynamic is fast. Conversely, it has the disadvantage that changes in temperature displace the resonant frequency and lead to discrepancies in the control. Rigorously, to avoid that inconvenience, an algorithm to track the resonant frequency should be implemented to anticipate the preload influence on the resonant frequency. Nevertheless we have chosen this approach, also easier to implement.

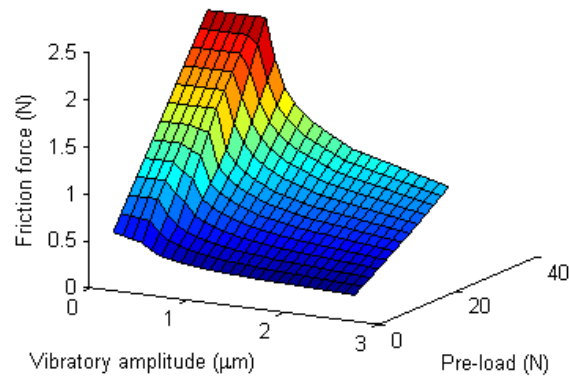


Figure 7. Friction force on the plate for a given tangential speed (simulation) as a function of the wave amplitude and the normal pre-load

7. Experimental set-up

To compare these theoretical results to the experimental ones, the set-up below was realised, and the friction force value has been measured.

The set up (Figure 8) involves a cable-driven pulley system used to pull the actuator by the mean of a DC motor Maxon at a defined controlled speed. Measuring current in the motor, we deduce the torque developed by the motor and then the force pulling the plate. An optical encoder is mounted on the rotating shaft to count motor speed and the set up is controlled by a dSPACE DS1104 card.

Under these conditions, Figures 9 and 10 finally show some results: especially, we have a friction force reduction which can reach 61.41% (from .71 N to .274 N for 3 N pre-load at 1 cm/s).

In Figure 9 a gap may be noticed between theoretical and experimental values in the case of a preload which equals 10 N. From an experimental point of view, it seems in that specific case, the friction reduction is not very acute. This may be attributed at a certain extent to a non linear variation of the tangential stiffness or to an additional mechanical phenomenon: a mechanical phenomenon such as the deformation of the substrate. However all these curves enable us to see that theoretical and experimental results are close especially for a preload less than 10 N, which tends to validate our model. More over, it may be noted that friction force is a function of the vibration. So, it may be controlled. We can also remark that this variation depends on the tangential speed imposed by the user and there will be a limitation of the effect for high speeds.

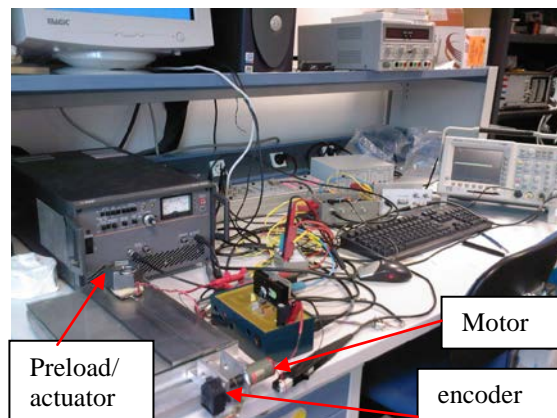


Figure 8. Experimental set-up

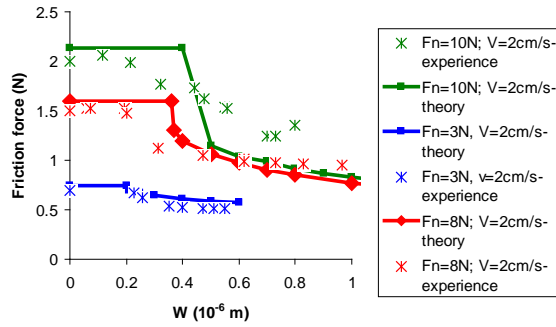


Figure 9. Theoretical and experimental results on steel surface; pre-load 3, 8 and 10 N, speed 2 cm/s

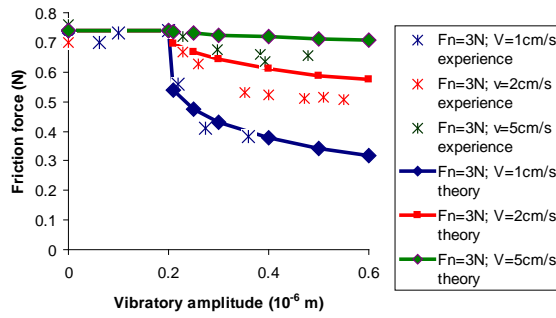


Figure 10. Theoretical and experimental results on steel surface; pre-load 3 N, speeds 1, 2 and 5 cm/s

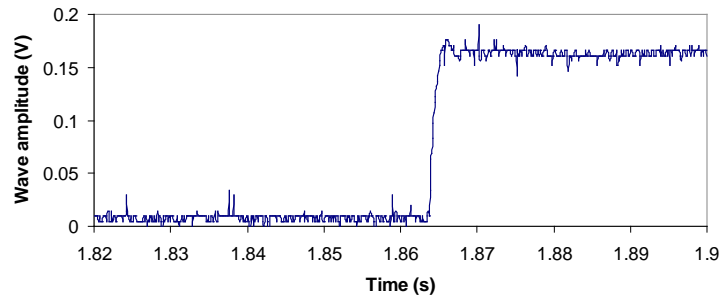


Figure 11. Wave amplitude response to a unit step reference

A last experiment has been carried out to check the accuracy of the wave amplitude control and in particular, the dynamic response time. In Figure 11, the plate response time in use with a pre-load on it is approximately 1 ms. According to the human mechano-receptor sensitivity and band-width (Pawluk and Howe, 1996), the changes induced on the friction force by the wave amplitude evolution will be well perceived.

8. Preliminary device evaluation

The evaluation method of a haptic device is often determined by the applications for which the device is dedicated. With devices working on the principle of friction reduction between two surfaces in contact, and from the famous Watanabe experience (Watanabe and Fukui, 1995), tactile interface designers check the accuracy of their device thanks to gratings exploration task. That is the case with Biet *et al.* (2008) and Winfield *et al.* (2007); both of them used friction variation of a surface to simulate various textures. Indeed it can be shown that under given conditions of frequency and vibratory amplitude, there's an excessive pressure (squeeze effect) in the air gap of two plates, one of the plates vibrating. In the works mentioned above, this principle has been used replacing one plate by the finger, the other one assuming the function of tactile device. In accordance with Watanabe experience, vibratory amplitude was correlated with friction reduction level between the fingertip and the plate. At last, when in contact with the vibrating plate, the finger feels a sliding sensation whilst without any vibration in the plate it's a sticky sensation which is perceived.

With our device, a temporal modulation of the friction coefficient at the foot/substrate interface was explored and it was found to produce more of a vibratory sensation rather than a texture. Then, we replaced the temporal modulation by a spatial one to feel a sensation close to texture perception. Like Biet and Winfield for tactile devices, we chose to simulate space fixed patterns shown on Figure 12, which induces a dependence relationship between exploration speed and texture pattern.

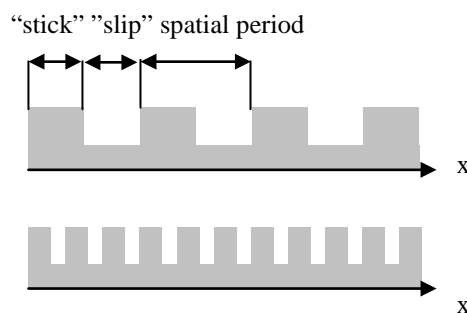


Figure 12. Two texture patterns with different spatial periods

To create anything like notches above, the idea is to generate alternatively sliding and blocking sensations, by tuning the vibrating wave amplitude. For that, it's sufficient to synchronise wave amplitude reference on the plate position moved by a user and measured by the optical encoder of the experimental setup. Therefore a spatio-temporal conversion defines the reference value for the friction force R_f , which is achieved by means of the wave amplitude control (Figure 13). By that way, sliding regions appear when the plate passes through the "holes" of the pattern depicted in Figure 12.

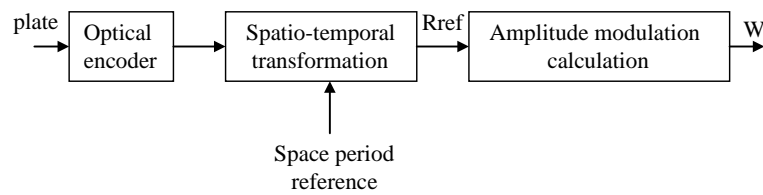


Figure 13. Control strategy in order to simulate texture patterns

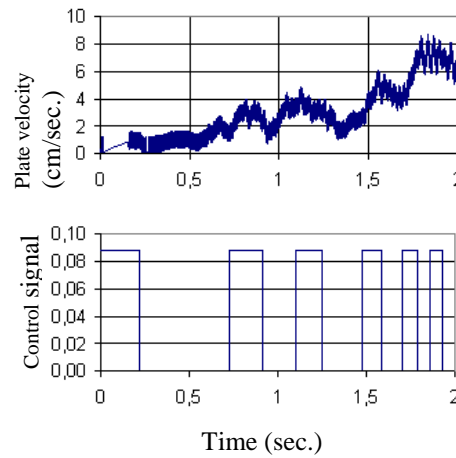


Figure 14. Influence of the displacement speed on the duration of stick-slip sequences

In order to illustrate the spatio-temporal modulation principle, we have plotted in Figure 14 the plate velocity (imposed by a user holding the plate in hand) as a function of time, as well as the control signal tuning the wave amplitude. In this case, we work with an on-off control: either the piezoceramics are supplied at the resonance frequency; either they are not supplied at all. In the first case, the friction

coefficient is reduced thanks to the lubrication effect, in the second one; the friction force corresponds to the dry friction force.

In Figure 14, we can see that an increasing of the displacement speed induces an increasing frequency of the control signals provided by the spatio-temporal transformation, in order to respect a given spatial period of the texture pattern.

9. Task and stimuli

Since there has not yet been defined a standard for meaningful haptic devices assessment, their evaluation implies specific tasks. These tasks also need to be simple enough to be easily applied while taking all important attributes of haptic interaction into account (West and Cutkowsky, 2003).

We will simulate the gratings depicted Figure 12 generated by the device along a given distance of 87 mm modifying randomly spatial frequency and vibration amplitude and counting spatial period present. This procedure is quite similar to that used by West and Cutowsky (West and Cutkowsky, 2003) who asked users to count the number of 1-D sinusoidal cycles on real and virtual surfaces.

The task required participants to move the plate on the steel substrate along the fixed distance (87 mm) and identify the number of cycles (space frequency in Figure 12) they perceive. Two groups (respectively two and five) of graduate students were chosen to perform the experiment. Results obtained with the first group were examined before conducting additional tests with the second group. One of the subjects was female.

The experimental setup was the one described in Figure 8 but this time, the plate was moved by the user himself instead of the DC motor. So, subjects performed self directed displacement of the plate forward and backward to familiarise with the manipulation. Next, they were instructed to grasp the pre-load plate and to move it without voltage supply. After what the plate was excited at their unknown. From this moment, they said they recognise kinds of jolts. Thereafter they knew the task consisted on counting the number of cycles present between the material limits of the displacement. We conducted some additional trials before starting the task. This stage took around 5 minutes. Participants used their dominant hand and made some comments at the end. The experiment lasted 30 minutes per participant.

10. Psychophysical results

To analyse the average results of the two groups of participants tested, we consider the absolute value of an average error rate (DER) defined as follows,

$$DER = \frac{(actual_cycles - cycles_detected)}{actual_cycles} \quad (9)$$

The average results obtained for both groups of subjects are graphically presented in Figure 15. We have plotted the average number of cycles detected for each given couple vibratory amplitude/grating spatial frequency. The symbol in the legend denotes the actual number of cycles imposed by the plate control for the corresponding test. Each curve tracks the results for a particular value of the spatial period (number of cycles present over departure and arrival lines), for different high frequency vibration amplitudes.

Figure 16 shows the average DER which is globally lower than 12%. It also shows the tendency toward an improvement of the spatial period perception when the vibratory amplitude increases. Finally, Figure 17 highlights the standard deviation on the mean value of DER for the participants. Once again, it may be noted that this deviation decreases as the vibration amplitude increases.

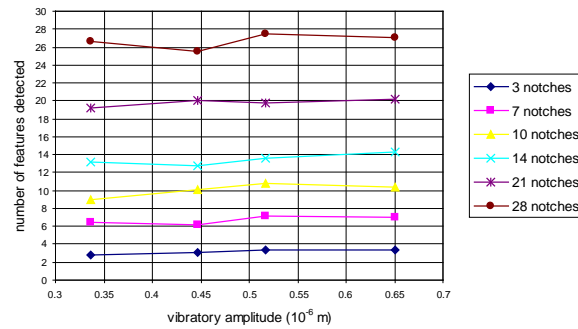


Figure 15. Average number of cycles detected as a function of wave amplitude for different values of the spatial period (notches)

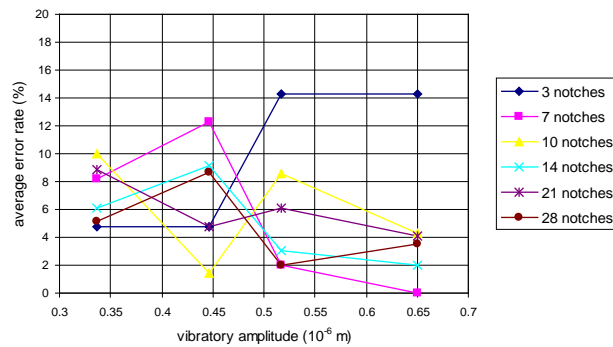


Figure 16. Average error rate as a function of wave amplitude for different values of the spatial period (notches)

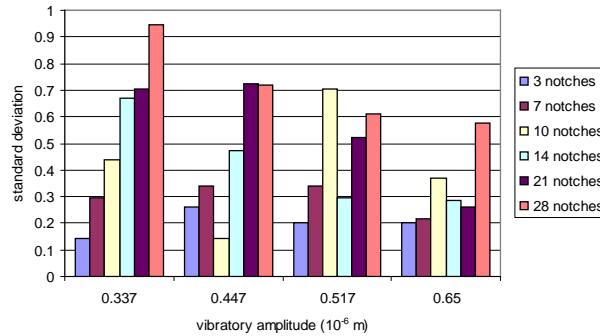


Figure 17. Standard deviation of error rate

11. Discussion

A counting experiment of gratings like regular jolts in a given distance has been conducted using the proposed device. Since some experimental parameters and the material differ from the one used by West and Cutowsky, we can not directly compare our results from theirs. Nevertheless, as they did, we used the DER to interpret our results. They considered a DER of 50% or more to be an indication that subjects were unable to count features accurately. These researchers considered the arbitrary limit of 50% confident with the comments from subjects about their perceived ability to count features. In the same way, in our experiment, the DER is globally less than 12% and participant comments did not vary. As a matter of fact, almost all the participants spontaneously stated firmly to feel a “strong” sensation when the higher vibratory amplitude (.65 μm on 1.7 μm available) was imposed.

12. Conclusion

In this paper, we propose to use the principle of active lubrication to design a 2 Dof passive haptic feedback device. The device is first described and its operating principle is explained as well. Then some details are given on the modelling of the device, leading to the expression of the tangential force. Simulations are performed in order to check the effectiveness of the friction control. According to an experimental set-up, those simulation results are successfully compared with the simulated ones. So, it is possible to control the friction force in a range available for force feedback rendering, even if this force highly depends on normal pre-load and tangential speed. First psycho-physic experiences have been conducted to evaluate this device in use. This preliminary evaluation trends to assess the validity of the interface for force feedback application.

Acknowledgement

This work has been carried out within the framework of INRIA Alcove project and is supported by IRCICA (Institut de recherche sur les composants logiciels et matériels pour l'information et la communication avancée).

Bibliography

- Biet M., Casiez G., Giraud F., Lemaire-Semail B. (2008). Discrimination of Virtual Square Gratings by Dynamic Touch on Friction Based Tactile Displays. *Symposium on Haptic Interfaces for Virtual Environments and Teleoperator Systems 2008*, 13-14 March, Reno, Nevada, USA.
- Casiez G., Plenacoste P., Chaillou C., Semail B. (2003). *Elastic Force Feedback With a New Multi-finger Haptic Device: The DigiHaptic*, Eurohaptics.
- Desai C.S., Zaman M.M. and Drum E.C. (1985). Cyclic Testing and Modelling of Interface. *J. of Geotech. Eng.* vol. 111, p. 793-815.
- Garbuio L., Rouchon J.F. (2006). Piezoelectric Thrust Bearing For Severe Environments, Actuator 2006, *10th International Conference On New Actuators*, 14-16 June, Bremen, Germany, p.185-188
- Le Moal P., Joseph E. Ferniot J.C. (2000). Mechanical energy transductions in standing wave ultrasonic motors: analytical modelling and experimental investigations. *European Journal of Mechanics A/Solids*, vol. 19, p. 849-871.
- Pawluk D., Howe R. (1996), A Holistic Model Of Human Touch. *Submitted to the 5th Annual C.N.S. Meeting*, Boston, MA.
- Piecourt E., Lajoie Mazenc M. (1995). *Electromechanical characterization and power supply of piezoelectric motors*, PhD thesis, Institut national polytechnique de Toulouse, Toulouse, France, n° 95 INPT 0102, 1995.
- Pigache F., Giraud F., Lemaire-Semail B. (2006). Modelling and identification of a planar standing wave ultrasonic motor. Identification of a planar actuator. *Eur. Phys. J. Appl. Phys.* 34, p. 55-65.
- Pigache F., Lemaire-Semail B., Giraud F., Bouscayrol A. (2005). Control of a piezo-electric actuator for adjustable brake in haptic devices. *EPE'05, DRESDE*, 11-14 September, CD-ROM ISBN 90-75815-08-05
- Samur E., Wang F., Spaetler U. and Bleuler H. (2007). Generic and systematic Evaluation of Haptic Interfaces Based on Testbeds, *Proc. Of the 2007 IEEE/RSJ International Conference on Intelligent Robots and Systems*, San Diego, CA, USA, Oct 29-Nov 2.
- Watanabe T., Fukui S. (1995). A method for controlling tactile sensation of surface roughness using ultrasonic vibration, *IEEE Int. Conf. on Robotics and Automation*, p. 1134-1139.
- West A. M., Cutkosky M.R. (2003). Detection of real and virtual fine surface features with a haptic interface and stylus, *ASME IMECE 6th Annual Symposium on Haptic Interfaces*, Dallas, TX, November.

Winfield L., Glassmire J., Colgate J. E., Peshkin M. (2007). T-PaD: Tactile Pattern Display through Variable Friction Reduction, *Second Joint Eurohaptics Conference and Symposium on Haptic Interfaces for Virtual Environment and Teleoperator Systems (WHC'07)*.

Received: 14 September 2012

Accepted: 25 March 2013